

Theory of the helical spin crystal: a candidate for the partially ordered state of MnSi

B. Binz,^{1,*} A. Vishwanath,¹ and V. Aji²

¹*Department of Physics, University of California, Berkeley, CA 94720, USA*

²*Department of Physics, University of California, Riverside, CA 92521, USA*

(Dated: March 23, 2022)

MnSi is an itinerant magnet which at low temperatures develops a helical spin density wave. Under pressure it undergoes a transition into an unusual partially ordered state whose nature is debated. Here we propose that the helical spin crystal (the magnetic analog of a solid) is a useful starting point to understand partial order in MnSi. We consider different helical spin crystals and determine conditions under which they may be energetically favored. The most promising candidate has bcc structure and is reminiscent of the blue phase of liquid-crystals in that it has line-nodes of magnetization protected by symmetry. We introduce a Landau theory to study the properties of these states, in particular the effect of crystal anisotropy, magnetic field and disorder. These results compare favorably with existing data on MnSi from neutron scattering and magnetic field studies. Future experiments to test this scenario are also proposed.

MnSi is a well studied itinerant ferromagnet [1] but has recently been at the focus of renewed attention since the discovery of unusual properties in high pressure studies [2, 3, 4, 5]. The ambient-pressure magnetic phase of MnSi is characterized by a hierarchy of three major energy scales [6]. First are interactions that favor itinerant ferromagnetism. At a much lower energy scale, Dzyaloshinskii-Moriya (D-M) spin-orbit coupling (which is allowed in the non-centrosymmetric B20 crystal structure of MnSi) leads to a spiraling of the magnetic moment with a single helicity (helical spin-density wave). The small ratio between these scales is responsible for the long spiral pitch ($\lambda = 180\text{\AA}$ vs. the lattice constant $a = 4.6\text{\AA}$). The D-M interaction defines chirality and the length of the ordering wave-vector ($Q = 2\pi/\lambda$) but not its direction. The latter is pinned to $\langle 111 \rangle$ by even weaker crystal-anisotropy terms [$\langle 111 \rangle$: class of crystal directions related by cubic symmetry]. Elastic neutron scattering at atmospheric pressure reveals Bragg spots at these eight points in the Brillouin zone which are attributed to domains each containing a single spiral state. On application of pressure however, a first order phase transition occurs at $p_c = 14.6\text{ kbar}$. At higher pressures, unusual properties are observed. First, the neutron scattering signal is completely changed from the low pressure phase. Enhanced scattering is seen at wavevectors with a length similar to the low pressure phase, but with intensities no longer sharply peaked along $\langle 111 \rangle$. Rather, the intensity is more diffuse over the wavevector sphere, hence the name "partial order", but clearly peaking at $\langle 110 \rangle$ [3]. Secondly, the resistivity displays a non fermi liquid (NFL) temperature dependence [4]. Although they both onset at p_c , the NFL persists to pressures far beyond where "partial order" is seen. The relation between these two puzzles is therefore unclear - here we focus only on offering a theory for the "partially ordered" state. Recent theoretical work on collective modes and electronic properties of helimagnets are in Refs. [7]. Other theoretical proposals for the high pressure state of MnSi

have invoked proximity to a quantum multi-critical point [8], magnetic liquid-gas transitions [9] and skyrmion-like structures [10, 11].

None of these theories has attempted to explain the new peak positions. As a first attempt, one might speculate that the crystal anisotropy which pins the spiral along $\langle 111 \rangle$ at low pressure is modified at high pressure and pins it along a different set of directions, $\langle 110 \rangle$. However, this view is untenable on many counts, e.g. it is at odds with the magnetic field studies [2]. Moreover, the usual crystal anisotropy terms consistent with the lattice symmetry give energy minima either at $\langle 111 \rangle$ or $\langle 100 \rangle$; but $\langle 110 \rangle$ are always saddle points (which can be proved more generally [12]). Similarly, while it is tempting to interpret the partially ordered phase of MnSi entirely in terms of a directionally fluctuating spin spirals, this requires both a novel theoretical framework for its description, as well as an explanation for the unusual anisotropy.

In this work, we study ordered magnetic states which are linear superpositions of spin spirals with different wave-vectors. We show that in addition to the three energy scales (ferromagnetic, D-M and crystal anisotropy) that are usually considered in MnSi, there is an additional scale that is important, the interaction between different modes (expected to be intermediate between the D-M and crystal anisotropy), which determines the spin crystal state that is selected. We propose that the transition under pressure between the single-spiral and partially ordered states is driven by a change in the inter-mode interactions that goes from preferring a single-spiral ground state to a multi-spiral ground state.

Magnetic weak crystallization theory: The Landau free energy to second order in the local spin density $\mathbf{M}(\mathbf{r})$ of a system with full rotation symmetry (transforming both space and spin together) - but no inversion symmetry is

$$F_2 = \langle r_0 \mathbf{M}^2 + J(\nabla \mathbf{M})^2 + 2D \mathbf{M} \cdot (\nabla \times \mathbf{M}) \rangle, \quad (1)$$

where $\langle \dots \rangle$ means averaging over the sample and r_0, J, D are parameters ($J > 0$). Coupling to fermions which

leads to damped dynamics is ignored in the following since we will focus on ground states with long range order. The last term of Eq. (1) is the D-M interaction. Clearly, the energy is minimal for circularly polarized waves of fixed helicity which satisfy $D \mathbf{m}_{\mathbf{q}}^* \cdot (i\mathbf{q} \times \mathbf{m}_{\mathbf{q}}) = -|D|q |\mathbf{m}_{\mathbf{q}}|^2$, where $\mathbf{m}_{\mathbf{q}}$ are the Fourier modes of $\mathbf{M}(\mathbf{r})$. Equation (1), then becomes $F_2 = \sum_{\mathbf{q}} r(q) |\mathbf{m}_{\mathbf{q}}|^2$, where $r(q) = r_0 - D^2/J + J(q - |D|/J)^2$. Here, in analogy to standard liquids (and in contrast to the uniform ferromagnetic case), $r(q)$ is minimized at a finite wavevector $Q = |D|/J$ and for $r(Q) \rightarrow 0$, all modes on the surface $|\mathbf{q}| = Q$ in reciprocal space become soft (as opposed to a single point $\mathbf{q} = 0$). To study the implications of such a singular surface on the phase transition itself is beyond the scope of this letter. But we recognize that when $r(Q) \rightarrow 0$, the Gaussian theory not only becomes unstable towards formation of a helical spin-density wave along any direction, but that linear combinations of such states (helical spin crystals) are equally natural candidates.

In the spirit of weak crystallization theory [13], we now study minima of the free energy in the ordered phase, where $r(Q) < 0$. The degeneracy between a simple spin spiral and linear combinations of several spin spirals (spin crystals) is lifted by interactions i.e. by the fourth-order term (F_4) in \mathbf{M} (odd terms in \mathbf{M} are forbidden by time reversal symmetry). We assume that F_4 , as F_2 , has full rotation symmetry and we will include the weak crystal anisotropy last. Hence, with $\mathbf{q}_4 = -(\mathbf{q}_1 + \mathbf{q}_2 + \mathbf{q}_3)$:

$$F_4 = \sum_{\mathbf{q}_1, \mathbf{q}_2, \mathbf{q}_3} U(\mathbf{q}_1, \mathbf{q}_2, \mathbf{q}_3) (\mathbf{m}_{\mathbf{q}_1} \cdot \mathbf{m}_{\mathbf{q}_2}) (\mathbf{m}_{\mathbf{q}_3} \cdot \mathbf{m}_{\mathbf{q}_4}). \quad (2)$$

If the interaction is strictly local in real space [$F_4 \propto \langle \mathbf{M}^4 \rangle$], which is equivalent to a constant coupling $U(\mathbf{q}_1, \mathbf{q}_2, \mathbf{q}_3) = U_0$, it is easy to show that the single-mode spin spiral is the absolute minimum of $F_2 + F_4$. In the spin spiral state, \mathbf{M}^2 is constant and it is therefore possible to minimize both F_2 and F_4 independently.

However, $U(\mathbf{q}_1, \mathbf{q}_2, \mathbf{q}_3)$ is generally not constant. Assuming F_4 is small, in that its main effect is to provide an interaction between the modes which are degenerate under F_2 , the important terms of F_4 are those with $|\mathbf{q}_1| = |\mathbf{q}_2| = |\mathbf{q}_3| = |\mathbf{q}_4| = Q$. Then the coupling function U depends only on two independent angles $2\theta = \arccos(\hat{\mathbf{q}}_1 \cdot \hat{\mathbf{q}}_2)$ and $\phi/2 = \arccos[(\hat{\mathbf{q}}_2 - \hat{\mathbf{q}}_1) \cdot \hat{\mathbf{q}}_3 / (1 - \hat{\mathbf{q}}_1 \cdot \hat{\mathbf{q}}_2)]$ [17]. This mapping allows θ and ϕ to be interpreted as the polar and azimuthal angles of a sphere and the coupling $U(\theta, \phi)$ is a smooth function on that sphere satisfying: $U(\theta, \phi) = U(\pi - \theta, \phi) = U(\theta, 2\pi - \phi)$. It is natural to expand U in spherical harmonics (Y_{lm}) which satisfy this relation and we just retain terms with $l \leq 2$. Thus $U(\theta, \phi) = U_0 + U_{11} \sin \theta \cos \phi + U_{20} (3 \cos^2 \theta - 1) + U_{22} \sin^2 \theta \cos 2\phi$.

To find the absolute minimum of $F_2 + F_4$ for a general angle-dependent interaction would be a formidable task. Instead, we first limit ourselves to linear combinations of six spin spirals, corresponding to wavevectors

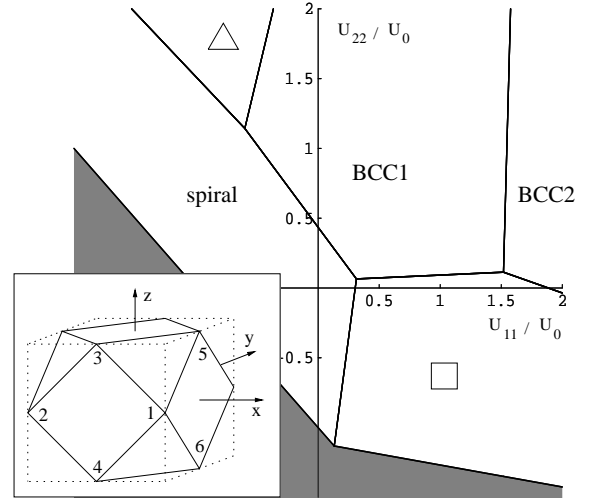


FIG. 1: Mean-field phase diagram of the six-mode model for $r(Q) < 0$ as a function of the interaction parameters for $U_{20} = 0$ and $U_0 > 0$. In the gray region, $F_4 < 0$ and higher-order terms should be added for stability.

$\pm \mathbf{k}_j$ (for $j = 1, \dots, 6$), where $\mathbf{k}_1 = Q/\sqrt{2}(1, -1, 0)$, $\mathbf{k}_2 = Q/\sqrt{2}(-1, -1, 0)$, etc. (see inset of Fig. 1). We may write the six modes as $\mathbf{m}_{\mathbf{k}_j} = \mathbf{m}_{-\mathbf{k}_j}^* = \psi_j \mathbf{n}_{\mathbf{k}_j}$, where $\mathbf{n}_{\mathbf{q}} = [\hat{\mathbf{q}} \times (\hat{\mathbf{z}} \times \hat{\mathbf{q}}) + i\hat{\mathbf{z}} \times \hat{\mathbf{q}}] / [1 - (\hat{\mathbf{z}} \cdot \hat{\mathbf{q}})^2]^{1/2}$. The choice of the unit vector $\hat{\mathbf{z}}$ is arbitrary. A different choice leads to a set of phase changes in the six complex variables ψ_j . The interaction Eq. 2, written in terms of the ψ -variables, contains terms of the form $V_{jj'} |\psi_j|^2 |\psi_{j'}|^2$ (three parameters) and one term $\lambda \Re(T_x + T_y + T_z)$, where $T_x = \psi_1^* \psi_2 \psi_5 \psi_6$, $T_y = \psi_1^* \psi_2^* \psi_3 \psi_4$ and $T_z = -\psi_3 \psi_4^* \psi_5^* \psi_6$ which is sensitive to relative phases. These are the only quartic terms invariant under the microscopic symmetries of the problem: translations, time reversal and tetrahedral point group operations. The parameters $V_{jj'}$ and λ can be easily expressed as a linear combination of U_0, U_{11}, U_{20} and U_{22} . The resulting mean-field phase diagram is shown in Fig. 1. Different ordered phases are separated by first-order phase boundaries. In the "spiral" state, only one out of six amplitude is non-zero. The square lattice state " \square " is a superposition of two orthogonal spin spirals with equal amplitude. In the region " Δ ", there are actually two degenerate states, one with $|\psi_i| > 0$ ($i = 1, 3, 5$) and one with ($i = 2, 4, 6$) (remaining amplitudes being zero in each case). Finally in BCC1 ($\lambda > 0$) and BCC2 ($\lambda < 0$), all six modes contribute with equal amplitudes. These states have the periodicity of a BCC crystal and will be the focus of this paper. Note that a small correction of the purely local interaction U_0 , given by $U_{11} \approx U_{22} \approx 0.2U_0$ is sufficient to induce a transition from the spiral state to the BCC1 spin crystal. [18]

Properties of the BCC spin crystal: From the sole assumption (suggested by experiments) that a spin texture has equal-weighted Bragg peaks at the set of wave-vectors

$\pm \mathbf{k}_j$, weak crystallization theory restricts an infinite variety of physically very different magnetization patterns $\mathbf{M}(\mathbf{r})$ down to only two possibilities: BCC1 and BCC2. In BCC1 (BCC2), the relative phases of ψ_1, \dots, ψ_6 are locked in such a way that T_x, T_y and T_z are all negative (positive), i.e. for BCC1: $\hat{\psi}_1 = \pm \hat{\psi}_4 \hat{\psi}_5$, $\hat{\psi}_2 = \mp \hat{\psi}_4 \hat{\psi}_6^*$, $\hat{\psi}_3 = \hat{\psi}_4 \hat{\psi}_5 \hat{\psi}_6^*$ where $\hat{\psi}_j = \psi_j / |\psi_j|$ and for BCC2: $\hat{\psi}_1 = \pm i \hat{\psi}_4 \hat{\psi}_5$, $\hat{\psi}_2 = \pm i \hat{\psi}_4 \hat{\psi}_6^*$, $\hat{\psi}_3 = -\hat{\psi}_4 \hat{\psi}_5 \hat{\psi}_6^*$. Three phases (e.g. $\hat{\psi}_4, \hat{\psi}_5, \hat{\psi}_6$) are arbitrary due to global translation symmetry. In addition to the translational degeneracy, both BCC states are two-fold degenerate due to time-reversal symmetry breaking. In contrast to the single spiral, time-reversal [$\mathbf{M}(\mathbf{r}) \rightarrow -\mathbf{M}(\mathbf{r})$] is *not* equivalent to a translation in either of the BCC states. In fact, both BCC states feature a macroscopic time-reversal symmetry breaking order parameter $S = \langle M_x M_y M_z \rangle \neq 0$.

BCC1 can be *defined* by its symmetry properties as being the unique structure that is invariant under time reversal (sign change of \mathbf{M}) followed by a $\pi/2$ rotation about the x, y or z axis. For BCC2, the same operations result in translations. The real space BCC1 structure is illustrated in Fig. 2. There are two sets of straight lines, along which \mathbf{M} is constrained by the symmetry properties of BCC1. First, the magnetization vanishes along the x, y and z axes [and their translations by $(\frac{1}{2}, \frac{1}{2}, \frac{1}{2})$], due to the invariance mentioned above. These are reminiscent of the blue phases of chiral nematic liquid crystals [14], where line defects also exist but are protected by topology, rather than by symmetry. Second, in the center between four parallel node lines, the magnetization direction is constrained as shown in Fig. 2 (a). Since these properties are determined by symmetry, they are stable, even if higher Fourier modes are included. In contrast, BCC2 has no node lines, but six point nodes in each primitive unit cell. Fig. 2 (c) shows the distribution of the local magnetization $|\mathbf{M}|$ over the sample.

Anisotropy and locking of crystal directions: So far, our model free energy [Eqs. (1) and (2)] has been completely rotation invariant. By choosing those six modes which lead to a BCC crystal, we assume that full rotation symmetry is spontaneously broken, but a global rotation still leaves the energy invariant. This degeneracy is broken by small anisotropic terms. For the MnSi B20 crystal structure, the leading anisotropic term in powers of M and q is of the form: $F_a = a \sum_j g(\hat{\mathbf{k}}_j) |\psi_j|^2$ where $g(\hat{\mathbf{k}}) = \hat{k}_x^4 + \hat{k}_y^4 + \hat{k}_z^4$. The function g has its maxima and minima along $\langle 100 \rangle$ and $\langle 111 \rangle$, respectively, while $\langle 110 \rangle$ is a saddle point. It is therefore impossible that this term locks a single-spiral to $\langle 110 \rangle$. From the observed spiral orientation along $\langle 111 \rangle$ at low pressures, we obtain $a > 0$. Assuming there is no sign change with pressure, we find that this locks the magnetic BCC crystal (BCC1 or BCC2) to the atomic B20 crystal in such a way that all $\hat{\mathbf{k}}_j$ point along $\langle 110 \rangle$. Hence it naturally explains the neutron scattering peaks at the locations seen in Ref. [3].

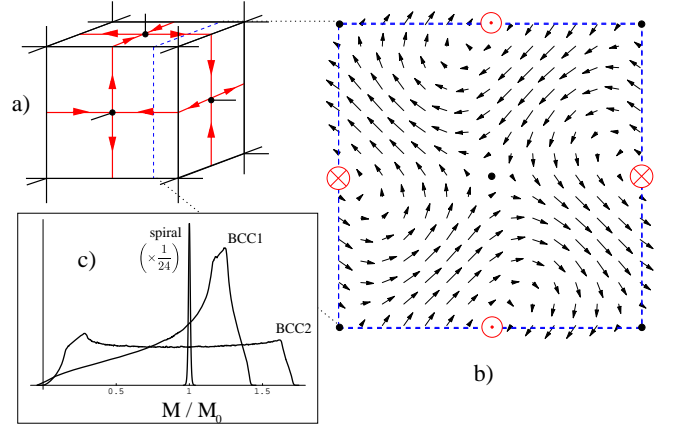


FIG. 2: (Color online) (a) Magnetization pattern $\mathbf{M}(\mathbf{r})$ of BCC1. The black lines are nodes, where $\mathbf{M} = 0$. Along red lines, the magnetization direction is as indicated. The blue dashed line indicates the location of the cut shown in (b) where vectors denote the in-plane magnetization. The nodes lines are the centers of anti-vortices and the directed red lines are the centers of meron configurations. (c) Probability distributions $\langle \delta(M - |\mathbf{M}(\mathbf{r})|) \rangle$ of three different magnetic states: a single-spiral state of amplitude M_0 and both BCC states with $|\psi_j|^2 = M_0^2/6$. Landau theory predicts this 1/6 ratio of amplitudes at the phase boundary between these states. A finite-width δ -function was used for the numerical evaluation.

Magnetic field: A uniform magnetic field couples linearly to the $\mathbf{q} = 0$ mode of the magnetization, $\mathbf{m} = \langle \mathbf{M} \rangle$. Eq. (2) couples this additional mode to the spin crystal modes and produces terms of the form $\mathbf{m}^2 |\psi_j|^2$, $(\mathbf{m} \cdot \hat{\mathbf{k}}_j)^2 |\psi_j|^2$ and one term $\mu \mathbf{h}_\psi \cdot \mathbf{m}$, where \mathbf{h}_ψ is cubic in the ψ variables [12]. The behavior of a single spin spiral in a magnetic field is characterized by a strongly anisotropic susceptibility, which effectively orients the spiral axis along the field [15]. Once the spiral is oriented, the susceptibility is comparatively large. In the BCC spin crystal states, there is no such anisotropy in the linear response, because symmetry does not allow for an anisotropic susceptibility tensor. Since the BCC spirals, unlike the single spiral, cannot be optimally oriented along the field, one expects the following sequence of phases as a function of increasing magnetic fields: “BCC” \rightarrow “spiral” \rightarrow “spin polarized”, in good comparison with experiment [2]. This expectation is true within our theory if μ is not too large. In fact, the term $\mu \mathbf{h}_\psi \cdot \mathbf{m}$ induces a change of the relative amplitudes and phases of the six interfering spirals as a function of the magnetic field and therefore adds to the ability of the BCC state to adjust to an external field. For example, a magnetic field in z -direction suppresses $|\psi_1|$ and enhances $|\psi_2|$ relative to the other four amplitudes [or the opposite, depending on the signs of μ and the time-reversal index $S = \langle M_x M_y M_z \rangle$]. This effect should be observable by neutron scattering in a single-domain sample, which may be obtained via

proper field-cooling. In practice this needs some care since the energy splitting between the two time reversed states is only cubic in the field: $\propto H_x H_y H_z$.

Magneto-transport: The broken time-reversal symmetry in the BCC spin crystals, but with the absence of a uniform magnetization, can give rise to unusual magneto-transport in single-domain samples. The symmetric part of the conductivity tensor is allowed a linear field dependence due to time reversal symmetry breaking ($S \neq 0$):

$$\sigma_{ab} = \sigma_0 \delta_{ab} + \alpha S |\epsilon_{abc}| H_c + O(H^2). \quad (3)$$

E.g. for a field applied along $\hat{\mathbf{z}}$, the conductivity along $(\hat{\mathbf{x}} \pm \hat{\mathbf{y}})/\sqrt{2}$ would display *linear* magneto-resistance. Similarly, the Hall conductivity (the antisymmetric part of σ) is allowed an unusual quadratic contribution:

$$\sigma_{ab}^H = \sigma_0^H \epsilon_{abc} H_c + \alpha' S \epsilon_{abc} |\epsilon_{cde}| H_d H_e + O(H^3). \quad (4)$$

Thus, the Hall effect will in general not simply switch sign if the direction of the magnetic field is inverted.

Effect of Disorder: Although the available MnSi crystals are very clean from the electrical resistivity point of view, helical magnetic structures are sensitive to disorder at a much longer length scale. Hence disorder effects need to be studied. Non-magnetic disorder which couples to the magnetization squared, $F_{dis} = \int d\mathbf{r} V_{dis}(\mathbf{r}) |\mathbf{M}(\mathbf{r})|^2$, will not affect single-spiral states which have a constant magnitude of magnetization, but they do affect spin crystal states which have a modulated magnitude [see Fig 2 (c)]. Therefore the neutron scattering signal of the spin-crystal state is expected to have more diffuse scattering than the single spiral, consistent with the experimental observation that the high pressure phase has diffuse scattering peaked about $\langle 110 \rangle$ while the low pressure phase has sharper spots. Anisotropic spreading of the Bragg spots parallel and perpendicular to the wavevector sphere is also anticipated [12]. Disorder in D=3 is expected to destroy true long range order of the spin crystal, leading to either a Bragg glass or a disordered state. In either case, time reversal symmetry breaking of BCC1 remains, implying that there must be a finite temperature phase transition on cooling into this phase.

NMR and μ SR: The spatially modulated magnetization magnitude of spin-crystal states [Fig. 2 (c)] should be visible in muon spin rotation (μ SR) and zero field NMR experiments. While μ SR on MnSi has been performed only at low pressures [16], zero field NMR was carried out over a wide range of pressure [5]. The resonant frequency was found to be sharp in the low pressure phase but to broaden at higher pressure. Both the presence of static magnetism and the broader distribution of frequencies ($|\mathbf{M}|$ distribution) is consistent with our proposal of BCC1 for the high-pressure phase.

Conclusions: A time reversal symmetry breaking helical spin crystal BCC1, disordered by weak impurities,

is proposed for the high pressure 'partially ordered' state of MnSi. Both theoretical arguments from simple models where this state naturally arises adjacent to the single spiral state, as well as favorable comparison with a variety of experiments: e.g. neutron scattering and magnetic field studies lends support to this view. Future experiments that could probe the unusual properties of this phase e.g. magneto-conductivity and μ SR are also proposed. Important puzzles that remain are the origin of NFL behavior and the lack of clear signatures for a finite temperature transition into the "partially ordered" state.

We thank L. Balents, I. Fischer, D. Huse, J. Moore, M.P. Ong, C. Pfleiderer, D. Podolsky, A. Rosch and T. Senthil for stimulating discussions; the Swiss National Science Foundation (B. B.), the A.P. Sloan Foundation and DE-AC02-05CH11231 (A.V.) for financial support.

* Electronic address: binzb@berkeley.edu

- [1] T. Moriya, *Spin Fluctuations in Itinerant Electron Magnetism* (Springer, Berlin 1985) and references therein.
- [2] C. Thessieu *et al.*, J. Phys.: Condens. Matter **9**, 6677 (1997).
- [3] C. Pfleiderer *et al.*, Nature **427**, 227 (2004).
- [4] C. Pfleiderer, S.R. Julian and G.G. Lonzarich, Nature **414**, 427 (2001); N. Doiron-Leyraud *et al.*, *ibid.* **425**, 595 (2003).
- [5] C. Thessieu *et al.*, J. Magn. Magn. Mater. 177-181, 609 (1998); W. Yu *et al.*, Phys. Rev. Lett., **92**, 086403 (2004).
- [6] O. Nakanishi *et al.*, Solid State Commun. **35**, 995 (1980); P. Bak and M.H. Jensen, J. Phys. C: Solid State Phys. **13**, L881 (1980).
- [7] S.V. Maleyev, Phys. Rev. B **73**, 174402 (2006); D. Belitz, T.R. Kirkpatrick and A. Rosch, *ibid.* **73**, 054431 (2006); S.V. Grigoriev *et al.*, *ibid.* **72**, 134420 (2005); I. Fischer and A. Rosch, Europhys. Lett. **68**, 93 (2004).
- [8] J. Schmalian and M. Turlakov, Phys. Rev. Lett. **93**, 036405 (2004).
- [9] S. Tewari, D. Belitz and T.R. Kirkpatrick, Phys. Rev. Lett. **96**, 047207 (2006).
- [10] U.N. Bogdanov, U.K. Rössler and C. Pfleiderer, Physica B **359-361**, 1162 (2005); cond-mat/0603103.
- [11] I. Fischer and A. Rosch (unpublished).
- [12] B. Binz and A. Vishwanath (in preparation).
- [13] S.A. Brazovskii, I.E. Dzyaloshinskii and A.R. Muratov, Sov. Phys. JETP **66**, 625 (1988) [Zh. Eksp. Teor. Fiz. **93**, 1110 (1987)].
- [14] D. C. Wright and N. D. Mermin, Rev. Mod. Phys. **61**, 385-432 (1989).
- [15] M. Kataoka and O. Nakanishi, J. Phys. Soc. Jpn. **50**, 3888 (1981); M.L. Plumer and M.B. Walker, J. Phys. C: Solid State Phys. **14**, 4689 (1981).
- [16] R. Kadono *et al.*, Phys. Rev. B **42**, 6515 (1990); R. Kadono *et al.*, *ibid.* **48**, 16803 (1993); I. M. Gat-Malureanu *et al.*, Phys. Rev. Lett. **90**, 157201 (2003).
- [17] Geometrically, $\phi/2$ is the angle between the two planes spanned by $(\mathbf{q}_1, \mathbf{q}_2)$ and $(\mathbf{q}_3, \mathbf{q}_4)$. If $\mathbf{q}_1 + \mathbf{q}_2 = 0$, $\phi/2$ is the angle between \mathbf{q}_2 and \mathbf{q}_3 .
- [18] We have also checked the energies of some spin crystal

states outside of the six-mode model [12]. The transition from the spin spiral to the BCC1 state remains stable

against all rivaling states tested so far.